Calculation of energy relaxation rates of fast particles by phonons in crystals

M. P. Prange, L. W. Campbell, D. Wu, F. Gao, and S. Kerisit

Phys. Rev. B **91**, 104305 — Published 20 March 2015

DOI: 10.1103/PhysRevB.91.104305

Calculation of energy relaxation rates of fast particles by phonons in crystals

M. P. Prange,[1,*] L.W. Campbell,[2] D. Wu,[1] F. Gao,[1,3] and S. Kerisit[1]

[1]*Fundamental and Computational Sciences Directorate, Pacific Northwest National Laboratory, Richland, WA 99354*
[2]*National Security Directorate, Pacific Northwest National Laboratory, Richland, WA 99354*
[3]*Department of Nuclear Engineering and Radiological Science, University of Michigan, Ann Arbor, MI 48109 USA*

We present *ab initio* calculations of the temperature-dependent exchange of energy between a classical charged point-particle and the phonons of a crystalline material. The phonons, which are computed using density functional perturbation theory (DFPT) methods, interact with the moving particle via the Coulomb interaction between the density induced in the material by phonon excitation and the charge of the classical particle. Energy relaxation rates are computed using time-dependent perturbation theory. The method, which is applicable wherever DFPT is, is illustrated with results for CsI, an important scintillator whose performance is affected by electron thermalization. We discuss the influence of the form assumed for quasiparticle dispersion on theoretical estimates of electron cooling rates.

PACS numbers: 63.20.kd,72.10.Di

I. INTRODUCTION

A unified quasiparticle picture of crystalline solids in which the physics of crystals is understood as a system of interacting electrons, holes, and phonons (and in some circumstances other types of quasiparticles like magnons) has become a universal way to understand interaction between crystals and external probes (*e.g.* photon, neutron, electron beams). Many experimental results can be predicted quantitatively using this picture, but some phenomena are described only qualitatively owing to an insufficient description of the quasiparticle properties or of their interactions. Often, analytic models based on model systems (*e.g.* the electron gas or the Hubbard model) with quasiparticles and interactions parametrized by a few numbers give a correct qualitative picture, but quantitative agreement requires fitting or numerical simulation. This work aims to make quantitative estimates based on a unified *ab initio* approach to the interaction between electrons and phonons in crystals. This interaction is well-understood qualitatively, but quantitative predictions from the standard picture rely on many untested and *ad hoc* assumptions.

The last decade has seen significant advances in the understanding of the microscopic physics and intrinsic performance limits of inorganic scintillators[1–10] which are used in a variety of contexts as spectroscopic radiation detectors. A feature of the emerging understanding of these systems is that variations in the spatial density of secondary excitations lead to non-proportionality of the scintillation signal to the energy of the exciting radiation, which in turn limits the achievable energy resolution of radiation detectors.[1,3–5,7,11] Detailed modeling based on Monte-Carlo methods,[12–14] pursued by the present authors and their collaborators, is shedding light on the microscopic processes occurring in scintillators. In this approach, an attempt is made to parametrize all the microscopic physical processes (*e.g.* photoabsorption, plasmon excitation by secondary electrons, exciton formation and diffusion, activator excitation and relaxation) that affect the transport of energy imparted to the scintillator by irradiation. These parameterizations are then used to simulate ensembles of scintillation events; the statistical distribution of the results is then interpreted as a theoretical prediction of the performance of real materials. Due to the dependence of scintillation non-proportionality on the spatial distribution of the excitations during scintillation, reliable theoretical predictions require a quantitative description of the dynamics of the excitations and thus rely heavily on an accurate treatment of electron-phonon interactions.

II. BACKGROUND

When a material undergoes high-energy excitation (*e.g.* by irradiation by photons or ions with energies up to MeV), the subsequent relaxation produces a large number of hot electrons and holes. If the material has a gap in the spectrum of electronic excitations, particles with kinetic energy smaller than the gap can not lose energy by electronic excitation. In this regime, the particles still exchange energy with the vibrational degrees of freedom. Although there has been a long history of scientific work on the electron-phonon interaction,[15–18] most treatments of the electron-phonon interaction focus on low energy carriers confined to a single band in small regions of **k**-space, which is natural in many contexts, such as superconductivity and low-energy transport, but is not sufficient for a faithful Monte-Carlo treatment of the thermalization phase. Therefore, the approach developed here is more general than these methods and provides a consistent treatment of the cooling of high- and low- energy particles by the lattice.

Frölich[15] made seminal contributions to our understanding of the electron-phonon interaction in the form

effects included	m^*	α
bare electron	1.0	5.44
band structure	0.312	3.13
polaron	1.9	7.50
polaron + band structure	0.593	4.31

TABLE I: Various plausible effective masses and corresponding Frölich coupling constants for electrons in CsI.

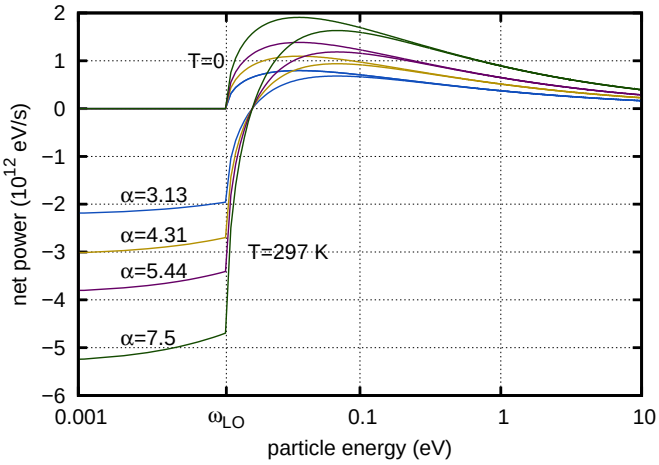

FIG. 1: (Color online) Power transferred to the longitudinal optical phonons in the Frölich model at zero (solid lines) and room (dashed lines) temperature with different coupling strengths α corresponding to different choices for the quasiparticle effective mass listed in Table I.

of a phenomenological treatment that follows from considering the macroscopic polarization induced by optical modes in polar crystals. A unified picture of the interaction of electrons with all modes was developed by Ziman[16] who assumed a (largely unspecified) independent-particle description of the electronic structure, in which the electrons in the solid occupy a collection of Bloch states $\psi_{\mathbf{k}}$, and derived expressions for the coupling of these orbitals by nuclear motion in the Born-Oppenheimer approximation. An account of this theory accessible to modern readers is given in the first chapter of Mahan.[19] The resulting formal theory remains the basis for most work on the electron-phonon interaction.[20,21] To use it to make quantitative predictions, the electron-phonon matrix elements must be estimated in some way.

To illustrate the difficulty posed by the unknown coupling strength, we consider the Frölich model in which the scattering rate and hence the transferred power are proportional to the dimensionless coupling constant $\alpha = \left(\frac{m^*}{2\omega_{\mathrm{LO}}}\right)^{1/2}\left(\frac{1}{\epsilon_\infty}-\frac{1}{\epsilon_0}\right)$. This model requires knowledge of the static and "high frequency" dielectric constants, ϵ_0 and ϵ_∞, as well as the effective mass m^* of the carrier being scattered. It is not clear exactly which effective mass should be used. A straightforward application of standard techniques (*i.e.* finding the self-energy to first order using perturbation theory and taking twice the imaginary part as the scattering rate) yields a model in which the mass appearing in the Frölich expressions is the band effective mass without renormalization by polaron effects. If one instead considers polaron quasiparticles (*i.e.* electrons dressed by phonon clouds) the same Frölich expressions are found but with the band effective mass replaced with the (greater) effective mass of the dressed polaron. The dependence on the effective mass in these models originates from a band picture of the crystal. As we discuss below, the description of the particle by an effective mass is inconsistent with modern, numerical knowledge of the actual quasiparticle band structure. In Table I, we list the values of these various effective masses for electrons in CsI. In Fig. 1, we plot the power exchanged between a particle and the lattice calculated for CsI with these different values for the effective mass. The lack of a clear prescription for selecting the appropriate effective mass leads to significant uncertainties in the power transferred and thus in predictions of the thermalization phase of scintillation.

Attempts to make realistic predictions for energy and momentum transfer were made by Sparks *et al.*[22] and Akkerman *et al.*[23] who used phenomenological arguments to parametrize and estimate the electron-phonon matrix elements. We are unaware of any more definitive work. For previous Monte-Carlo simulations,[12–14] we have developed models for the cooling of electrons by phonons based on this type of work.[15,22–24] With the current work, we aim to reduce the amount of *ad hoc* assignments involved in this estimation by resorting to DFT electronic structure calculations for the strength of the interaction directly.

In order to find a workable and quantitative method to estimate the exchange of energy between phonons and charged particles, we have developed a semi-classical theory in which the field of a charged particle (moving with a specified velocity) is treated as a perturbation to the vibrational modes of the crystal and present numerical calculations of the power transferred between the lattice and perturbing charge that are based on density functional perturbation theory calculations of the density response to lattice distortions. We have chosen a classical description of the particle to maintain compatibility with our scintillator simulations.[12–14,25,26] This approach is preferable because a wave-packet description of a particle in the Bloch picture requires the spatial extent of the region in space at which the particle might be measured to contain many unit cells (so that the packet can be limited to a relatively small region in **k**-space) while we want to model the interaction of the particle with point defects (*e.g.* activators) that are situated at certain definite positions. These models will invariably involve the distance between the particle and the point defect, leading to ambiguity if the particle wave packet is large compared to the unit cell. Although the difference between quantum and classical descriptions of the particle that is being scattered is conceptually stark, the

resulting expressions for phonon scattering have the same form. Thus a close analogy between the classical theory presented here and the traditional quantum picture can easily be drawn by equating the coefficients of the energy- and momentum-conserving δ-functions. When viewed in this light, the present work amounts to fixing the *ad hoc* interaction strengths in the old models with DFT calculations. We also remark that the correspondence of quantum and classical descriptions suggests that, as far as the energy relaxation is concerned, details of the wave-packet in the quantum description probably are not important.

III. SEMICLASSICAL TREATMENT OF THE ELECTRON-PHONON INTERACTION

In this manuscript we present a model in which a classical charged particle interacts with a quantized phonon system. The properties of the phonon system are derived using adiabatic Born-Oppenheimer dynamics in the harmonic approximation. The interaction Hamiltonian is taken as the instantaneous Coulomb interaction and hence neglects retardation, transverse effects, etc. These approximations for the phonons are standard and discussed by many authors.[16,17,19] The classical treatment of the perturbing charge is nonstandard. For example, the perturbing particle is not described in terms of the band structure of the host material and is simultaneously assigned a precise position and momentum.

We denote an arbitrary point in momentum space with $\mathbf{q}+\mathbf{G}$ where $\mathbf{q}$ is from the first Brillouin zone and $\mathbf{G}$ is from the reciprocal lattice. We use Hartree atomic units ($e^2=\hbar=m=1$). We analyze a model of the interaction of a crystal with an external point particle of charge Z at a time-dependent position $\mathbf{r}(t)$. The fundamental quantities in this analysis are the positions $\{\mathbf{R}_{s,\kappa}(t)\}$ of the nuclei of the atoms that comprise the crystal. The subscript s refers to the unit cell and κ refers to the sublattice which hosts nuclei of charge Z_κ. The crystal has N repeated unit cells which occupy a volume $V=N\Omega$. These nuclear positions (and their conjugate momenta) are quantum mechanical operators; the Hamiltonian of our theory is the kinetic energy of the nuclear motion plus the ground state potential energy surface which depends only on the nuclear positions. As the perturbing particle moves through the lattice, it exerts forces on the crystal, which responds by deforming. We assume the interaction energy is given by

$$H_{\rm int}(t) = Z\int d^3r' \, \frac{\delta n_{\rm tot}\left(\mathbf{r}'\right)}{\left|\mathbf{r}(t)-\mathbf{r}\,'\right|}, \tag{1}$$

where

$$\begin{aligned}\delta n_{\rm tot}\left(\mathbf{r}\right) &= \delta n_{\rm nuc}\left(\mathbf{r}\right)+\delta n_{\rm elec}\left(\mathbf{r}\right)\\ &= \sum_{s,\kappa} Z_\kappa\left[\delta^3\left(\mathbf{r}-\mathbf{R}_{s,\kappa}\right)-\delta^3\left(\mathbf{r}-\mathbf{R}^{(0)}_{s,\kappa}\right)\right]\\ &\quad -\left[n\left(\mathbf{r};\{\mathbf{R}_{s,\kappa}\}\right)-n\left(\mathbf{r};\left\{\mathbf{R}^{(0)}_{s,\kappa}\right\}\right)\right]\end{aligned} \tag{2}$$

is the change in the ground state charge density of the crystal (electrons and nuclei) induced by displacing the nuclei from their equilibrium positions $\left\{\mathbf{R}^{(0)}_{s,\kappa}\right\}$ to positions $\{\mathbf{R}_{s,\kappa}\}$.

We write the Hamiltonian for our model in terms of annihilation and creation operators for phonon modes:

$$\begin{aligned}H &= H_0+H_1\\ &= \sum_{\lambda,\mathbf{q}}\omega_{\lambda,\mathbf{q}}\left(a^\dagger_{\lambda,\mathbf{q}}a_{\lambda,\mathbf{q}}+\frac{1}{2}\right)+\sum_{\lambda,\mathbf{q}}H_{\lambda,\mathbf{q}}(t)\left(a^\dagger_{\lambda,-\mathbf{q}}+a_{\lambda,\mathbf{q}}\right).\end{aligned} \tag{3}$$

In the sums here, $\mathbf{q}$ runs over the Brillouin zone of the crystal and λ over the phonon branches of which there are three times the number of sublattices. The energy of branch λ at wavevector $\mathbf{q}$ is $\omega_{\lambda,\mathbf{q}}$. The time dependent coupling

$$H_{\lambda,\mathbf{q}}(t) = \sum_{\mathbf{G}}\frac{(4\pi Z)}{\left|\mathbf{q}+\mathbf{G}\right|^2}n_\lambda\left(\mathbf{q}+\mathbf{G}\right)e^{i(\mathbf{q}+\mathbf{G})\cdot\mathbf{r}(t)} \tag{4}$$

is the Coulomb interaction between the charge density $n_\lambda\left(\mathbf{q}+\mathbf{G}\right)$ induced at wavevector $\mathbf{q}+\mathbf{G}$ by excitation of the phonon mode $(\mathbf{q},\lambda)$ (which has annihilation and creation operators $a_{\lambda,\mathbf{q}}$ and $a^\dagger_{\lambda,\mathbf{q}}$) and the charge density $Ze^{i(\mathbf{q}+\mathbf{G})\cdot\mathbf{r}(t)}/V$ of the perturbing particle, which has charge Z and is moving through a crystal with volume V.

To complete the theory, the induced density $n_\lambda\left(\mathbf{q}+\mathbf{G}\right)$ must be specified. We do so in the context of density functional perturbation theory (DFPT) in a plane wave setting.[27,28] This choice yields *ab initio* predictions based on detailed electronic structure calculations and distinguishes the current work from previous efforts which relied on *ad hoc* forms for the electron-phonon interaction.

IV. COMPUTATIONAL METHODS

A. Integral to evaluate

Within DFPT, the ground state energy of the crystal and attendant quantities like the Kohn-Sham orbitals and the electronic density are expanded in powers of the strength of a perturbation applied to the crystal system. For phonon physics, the relevant perturbations are displacements of the nuclei and the application of a homogeneous electric field. A great advantage of DFPT is that these perturbations do not have to be commensurate with the crystal ground state, and calculations at arbitrary wave vectors can be accomplished without constructing a supercell commensurate with the perturbation. In practice, we use the ABINIT code[27–30] to construct the first-order density response $n^{(1)}_{\kappa,i,\mathbf{q}}$ to small displacements of each sublattice κ along each crystal axis i on a regular grid of points $\mathbf{q}$ in the Brillouin zone. (For each $\mathbf{q}$

the cell-periodic response is output in real space; we use fast Fourier transform routines to convert them to momentum space.) The same calculations yield the phonon band structure and the eigenvectors of the dynamical matrices that characterize the motion of the various atoms in the crystal when a phonon mode is excited. These methods are described in Ref. [27].

In order to make predictions useful for modeling the dynamics of charged particles traversing the crystal, we have taken these ingredients from DFPT and computed the rate of change of the energy stored in the phonon system using perturbation theory applied to Eqs. 3 and 4. Using second-order time-dependent perturbation theory and assuming that the perturbing particle's kinetic energy is given in terms of its velocity $\mathbf{v}$ by $v^2/2$ we find (after averaging over positions of the perturbing particle at time $t = 0$) the following expression for the rate of excitation (upper sign) or deexcitation (lower sign) of the $\lambda, \mathbf{q}$ phonon mode:

$$\Gamma^{(\pm)}_{\lambda,\mathbf{q}} = \frac{2\pi N}{V} \sum_{\mathbf{G}} \left| \frac{4\pi Z n_\lambda(\mathbf{q}+\mathbf{G})}{(\mathbf{q}+\mathbf{G})^2} \right|^2 \delta\left(\pm\omega_{\lambda,\mathbf{q}} - (\mathbf{q}+\mathbf{G})\cdot\mathbf{v} + \frac{1}{2}(\mathbf{q}+\mathbf{G})^2 \right). \tag{5}$$

This equation has the form of a sum over channels (in this case the Fourier component $\mathbf{q}+\mathbf{G}$ of the induced density) of a coupling strength times an energy conserving delta-function. The sum is incoherent: the square of the interaction Hamiltonian is taken before summing over Fourier components. This feature results from averaging over trajectories with the same velocity. It is interesting to note that Eq. 5 can also be obtained from a quantum description of the scattered particle in which the unperturbed eigenstates are plane waves $e^{i\mathbf{k}\cdot\mathbf{r}}/V^{1/2}$ with energies $k^2/2$.

An explicit expression for the induced density is

$$n_\lambda(\mathbf{q}+\mathbf{G}) = \sum_{\kappa,i} \frac{u^*_{\kappa,i,\lambda}(\mathbf{q})}{\sqrt{2M_\kappa \omega_{\lambda,\mathbf{q}}}} \left(\tilde{n}^{(1)}_{\kappa,i}(\mathbf{q}+\mathbf{G}) - iZ_\kappa e^{-i\boldsymbol{\tau}_\kappa\cdot(\mathbf{q}+\mathbf{G})}(\mathbf{q}+\mathbf{G})\cdot\hat{\mathbf{x}}_i \right), \tag{6}$$

where Z_κ, M_κ, $\boldsymbol{\tau}_\kappa$ are the charge, mass, and location in the first unit cell of the atoms occupying the κ^{th} sublattice. The first term in parentheses in Eq. 6 is the electronic response; the second is the nuclear response. The phonon quantities $\tilde{n}^{(1)}_{\kappa,i}$, $u_{\kappa,i,\lambda}$, and $\omega_{\lambda,\mathbf{q}}$ are respectively the induced density, phonon eigenvector, and phonon energy (band structure). All of these are taken directly from the ABINIT output; i denotes the direction in which the atoms move, and $\hat{\mathbf{x}}_i$ is a unit vector in this direction. To avoid infrared divergences in the scattering rate for acoustic phonons, we evaluate the power $P_{\text{rad}} = \sum_{\lambda,\mathbf{q}} \omega_{\lambda,\mathbf{q}} \Gamma_{\lambda,\mathbf{q}}$ transferred to the lattice by the perturbing particle instead of the scattering rate.

We can also consider the rate of scattering for a particle moving through the crystal whose phonon modes are in thermal equilibrium at a given temperature T. In this case the power transmitted from the perturbing particle to the crystal, averaged over a thermal ensemble of systems, is

$$\langle P_{\text{rad}} \rangle = \sum_{\lambda,\mathbf{q}} \omega_{\lambda,\mathbf{q}} \left[(N(T,\omega_{\lambda,\mathbf{q}})+1)\,\Gamma^{(+)}_{\lambda,\mathbf{q}} - N(T,\omega_{\lambda,\mathbf{q}})\Gamma^{(-)}_{\lambda,\mathbf{q}} \right], \tag{7}$$

where

$$N(T,E) = \left(e^{E/(k_B T)} - 1 \right)^{-1} \tag{8}$$

is the Bose occupation factor (k_B is the Boltzmann constant). Eq. 7 is the expression we wish to evaluate.

B. Tabulation of the scattering potential

We have developed a computer program to complete the evaluation of Eq. 7 as a function of temperature and the velocity of the perturbing particle. The program first computes and tabulates (on the plane wave grid inherited from ABINIT and a regular grid of $\mathbf{q}$-points spanning the irreducible Brillouin zone) in a binary file the combination

$$\frac{2\pi N}{V} \left| \frac{4\pi Z n_\lambda(\mathbf{q}+\mathbf{G})}{(\mathbf{q}+\mathbf{G})^2} \right|^2 \tag{9}$$

that appears in Eq. 5. We call this quantity the scattering potential.

Since the scattering potential is ill-defined at the origin, we employ a special treatment of the Γ-point to find the first-order induced dipole moment that is based on the first-order orbitals at Γ. One can derive a multipole expansion for the induced density by expanding the exponential $e^{-i\mathbf{q}\cdot\mathbf{r}} = 1 - i\mathbf{q}\cdot\mathbf{r} + \cdots$ involved in the Fourier transform of the induced density. Each term in this expansion gives rise to a multipole tensor. The monopole term vanishes because the total charge of the system is fixed (the phonons simply move around existing charges). Similarly, when a long-wavelength acoustic phonon is excited, the crystal experiences a uniform translation in space. Since the density is rigidly translated, there is no induced dipole moment for long-wavelength acoustic modes. We calculate the first-order density near $\mathbf{q} = 0$ using

$$i\tilde{n}^{(1)}_{\kappa,i,\mathbf{q}} \approx \mathbf{q}\cdot \left[\sum_\alpha^{\text{occ}} \int_{\Omega_0} d^3r\, \psi^{(0)}_\alpha \boldsymbol{\nabla} \psi^{(1)}_{\alpha,\kappa,i,\mathbf{q}=\mathbf{0}} - \psi^{(1)}_{\alpha,\kappa,i,\mathbf{q}=\mathbf{0}} \boldsymbol{\nabla} \psi^{(0)}_\alpha + c.c. \right]. \tag{10}$$

Here α denotes the band and crystal momentum of an occupied orbital $\psi^{(0)}_\alpha$ in our calculation of the ground state of the crystal, and $\psi^{(1)}_{\alpha,\kappa,i,\mathbf{q}=\mathbf{0}}$ is the corresponding first

order orbital (output in the 1WF files by ABINIT) resulting from a uniform displacement of the κ sublattice in the i^{th} direction. The vector in square brackets in Eq. 10 is tabulated for all the combinations of i and κ and saved to disk. In this step, we assure that the dipole moment induced by a rigid translation of the crystal vanishes by shifting the dipole expansion coefficients for all sublattice by the same amount. This is numerically necessary since

$$\int \frac{d^3q}{(2\pi)^3} q^{-n} \delta\left(\alpha q + \mathbf{q}\cdot\mathbf{v} + q^2/2\right) \tag{11}$$

diverges for $n \geq 3$, and any small dipole moment induced by the excitation of a long-wavelength acoustic mode (with energy αq) will lead to divergence in the calculated power.

During the course of the integration the value of the scattering potential for a given phonon mode is required at arbitrary points in momentum space. We use linear interpolation of the tabulated values of Eq. 9 when none of the tabulated points involved in the interpolation is $\mathbf{q} = \mathbf{G} = \mathbf{0}$. Otherwise, we assign the origin the value of the scattering potential deduced from the dipole expansion Eq. 10. This gives interpolated results that become identical to the dipole expansion near the origin and smoothly change over to direct linear interpolation outside the first shell of points in the $\mathbf{q}$-grid.

C. Adaptive integration for the transferred power

With the scattering potential and dipole expansion coefficients tabulated, Eq. 7 can be evaluated. To do so, we employ an adaptive integration method based on the tetrahedron method. The delta-function in Eq. 7 enforces conservation of energy and momentum on the emission and absorption of phonons: the scattering processes that contribute to the transferred power all lie on the kinematically allowed surface defined by

$$\begin{aligned} 0 =& \pm\omega_{\lambda,\mathbf{q}} - (\mathbf{q}+\mathbf{G})\cdot\mathbf{v} + \frac{1}{2}(\mathbf{q}+\mathbf{G})^2 \\ =& \frac{1}{2}\left[\mathbf{v} - (\mathbf{q}+\mathbf{G})\right]^2 \pm \omega_{\lambda,\mathbf{q}} - \frac{\mathbf{v}^2}{2} \\ =& E_f - E_i \end{aligned} \tag{12}$$

where E_f and E_i are the energies after and before the collision respectively. Our iterative integration method is based on integration over cubes in $\mathbf{q}+\mathbf{G}$ space. For a given velocity of perturbing particle and phonon branch, we start our procedure with eight cubes chosen to enclose the kinematically allowed surface. Each cube has one corner at the particle velocity. Since the RHS of Eq. 12 attains its minimum at $\mathbf{q}+\mathbf{G} = \mathbf{v}$, these corners are inside the kinematically allowed surface if Eq. 12 has a solution. The side length of these eight cubes is chosen so that the RHS of Eq. 12 is positive for all other (exterior) cube corners. This guarantees that three faces of each cube intersect the kinematically allowed surface if it exists. The cubes are decomposed into tetrahedra. The contribution to the integral Eq. 7 is then computed for each of these using standard techniques.[31] The program now has a list of cubes and a current (generally very poor) approximation of the contribution of each cube to the desired integral.

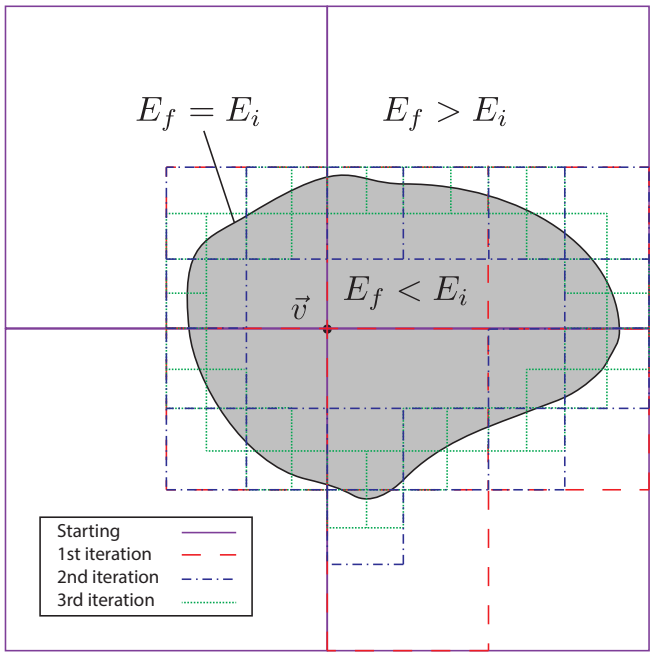

FIG. 2: (Color online) Schematic drawing of cubes used in the adaptive integration scheme. In this two-dimensional analogy, the cubes are represented by squares and the volume circumscribed by the kinematically allowed surface is shaded in gray. The initial cubes (purple solid lines) all share a common vertex at the particle velocity, and all other vertices are outside the kinematically allowed surface. The 7 cubes resulting from the first subdivision (red dashes), the 17 cubes resulting from the second subdivision (blue dash-dots), and the 38 cubes resulting from the third subdivision (green dots) are also shown.

The program then proceeds iteratively by considering the first cube on the list. This cube is subdivided into eight daughter cubes, and the integral is estimated in each of these that intersects the kinematically allowed surface using the tetrahedron method. If the sum of the integrals over the daughter cubes is within tolerance of the previous estimate for the parent cube, this contribution is accumulated and the cubes are discarded from the list. If the estimate from the subdivided cubes differs from the previous one by more than the tolerance, the parent cube is replaced on the list by its contributing daughters, and the integration continues with the daughter cubes at the top of the list. Eventually the cube list is exhausted and the accumulated result is the final value of the integral. The cubes involved in the first few iterations are schematically illustrated in Fig. 2. This procedure has been found to give good numerical results for models (*e.g.* the Frölich model) for which analytic results are

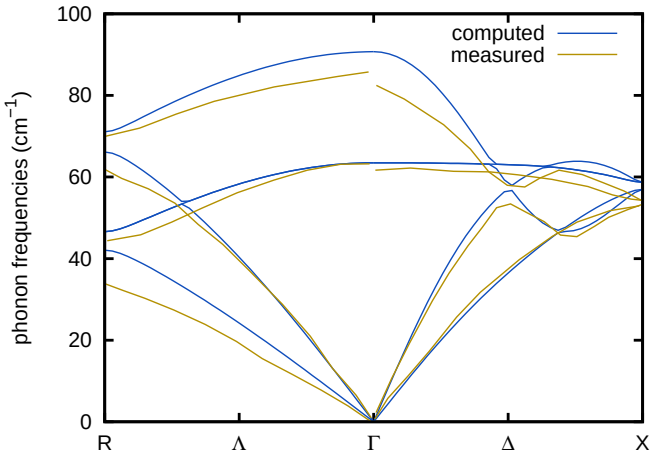

FIG. 3: (Color online) Computed phonon band structure along [111] and [100] directions in CsI compared to measurements taken from Ref. [34].

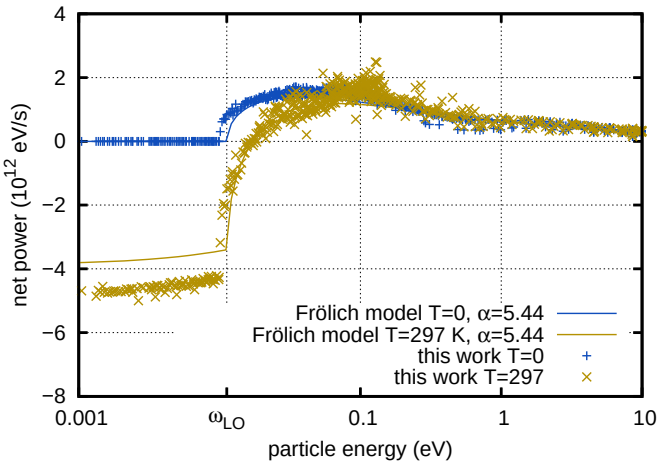

FIG. 4: (Color online) Computed power transferred by the longitudinal optical phonons compared to the Frölich model with coupling strength $\alpha = 5.44$ (appropriate for electrons with vacuum electron mass $m^* = 1$ in CsI).

available.

V. RESULTS AND DISCUSSION

We have completed calculations using these methods for the ionic scintillator CsI. As mentioned above, the phonons are computed using the ABINIT code. We used norm-conserving pseudopotentials of the Troullier-Martins[32] type obtained from the ABINIT website for all calculations presented here. The LDA parametrization of Goedecker, Teter, and Hutter[33] was used.

For CsI, a $12\times12\times12$ regular grid (resulting in 84 symmetry inequivalent points) of points in the Brillouin zone was employed for both the electronic and phonon structures. The energy cutoff was set at 20 Ha. The resulting phonon band structure is plotted in Fig. 3. It is seen to be in good agreement with the measured[34] phonon spectrum. Our calculations find the longitudinal-optical phonon mode at Γ to have frequency $4.13\times10^{-4}\,\mathrm{Ha} = 0.0112\,\mathrm{eV} = 90.7\,\mathrm{cm}^{-1}$. This energy has been labeled ω_{LO} in Figs. 4, 5, and 7. The phonon eigenvectors and first-order induced densities were printed out. At Γ, the first-order wave functions were also printed out.

These ingredients were then used as described in Section IV to compute the rate of energy transfer between particles and the lattice at $\simeq$ 1000 randomly selected velocities $\mathbf{v}$ such that the corresponding kinetic energy is less than 10 eV (corresponding to the energy range over which phonons might play a significant role in energy transfer in CsI). The contributions to the transferred power by the LO mode are plotted in Fig. 4 at zero and room temperatures. Also plotted in that figure is the Frölich model for $m^* = 1$ (the $\alpha = 5.44$ trace from Fig. 1).

We plot the contributions to the transferred power by the acoustic modes in Fig. 5. The *ab initio* room temperature results are noisier than corresponding results for the optical modes. We have added smooth lines (using gnuplot's bezier smoothing) through the calculated results in figures where appropriate. This variation comes from dependence of the results on the direction of the velocity (we use velocities randomly chosen from a uniform angular distribution). The small (vanishing in the small q limit) phonon frequencies near the zone center give rise to large Bose occupation factors and hence large rates of stimulated absorption and emission of phonons (terms proportional to $N(T,\omega_{\lambda,\mathbf{q}})$ in Eq. 7). Since these terms largely cancel, the difference of these terms in Eq. 7 has large fractional variation. We plot the contributions to the total power from stimulated absorption and emission (and their difference) in Fig. 6.

Examination of Fig. 5 shows that our *ab initio* estimates have much more energy exchanged through the acoustic modes, especially at low energies, than the previously used phenomenological model (again we show the phenomenological model for $m^* = 1$ but the conclusion is not changed by the use of any reasonable effective mass). At representative particle velocities (*e.g.* the particle kinetic energy is half of the band gap) the power removed from the particle by acoustic modes is several times larger than that removed by the LO modes. This is opposite to the behavior of the Sparks[22] model. The more efficient cooling by acoustic modes leads to overall greater transferred power as seen in Fig. 7, which shows our total computed results (including all phonon branches throughout the Brillouin zone) compared to our previous model.[13] There is more energy transferred, and it mostly goes through the acoustic modes.

Bardeen and Shockley[35] pioneered the usual approach to electron interactions with acoustic phonons with the introduction of deformation potential (*i.e.* the change in the band structure induced by local changes in lattice

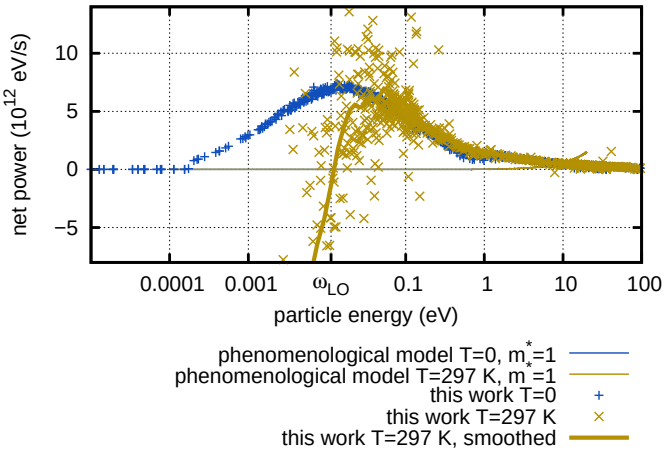

FIG. 5: (Color online) Computed power transferred by the longitudinal acoustic phonons compared to the phenomenological model of Ref. [13] evaluated with the vacuum electron mass $m^* = 1$. Our *ab initio* estimates are much larger than the phenomenological model at all energies of interest.

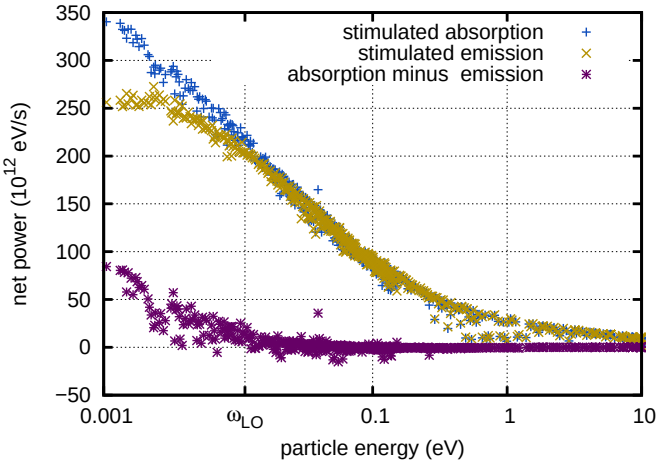

FIG. 6: (Color online) Contributions to the transferred power at T=297 K by stimulated processes.

parameter accompanying acoustic phonon excitation), which can be closely related to the elastic constants of the material. This picture is based on the assumption of a delocalized electron that can only interact with the $\mathbf{G} = \mathbf{0}$ component of the scattering potential (Umklapp processes are forbidden). Our model is a complementary picture in which the particle is assumed to be a classical point charge with no spatial extent. Such a particle is much more likely to scatter from the variations in the potential within the unit cell.

All of the theories of electron-phonon scattering discussed here have the familiar form (displayed in Eq. 5), in which each loss channel contributes to the scattering from a given initial state to each kinematically allowed final state by an amount equal to the strength of coupling of the initial and final states (in the current work this coupling strength is Eq. 9). If the strength of the electron-phonon interaction does not depend on the particle velocity (*e.g.* if the instantaneous Coulomb interaction is used, as is done in all the models discussed here), the particle dispersion enters only through kinematical constraints (*i.e.* conservation of energy and momentum). Knowledge of two physical properties is needed to make useful predictions: the interaction strength (which determines the magnitude of the factor multiplying the δ-function) and the kinematics of a collision between an electron and phonon (which determines the zeros of the δ-function argument). Our understanding of electrons and phonons is based on standard models[15–19,22–24,36,37] which assume effective mass dispersion. In this work we have replaced semi-phenomenological and *ad hoc* assumptions about the interaction strength with *ab initio* calculations, finding that it is stronger than the interaction in the standard models. Our use of classical dispersion for the particle that is being scattered is equivalent to the normal effective mass approximation for dispersion.

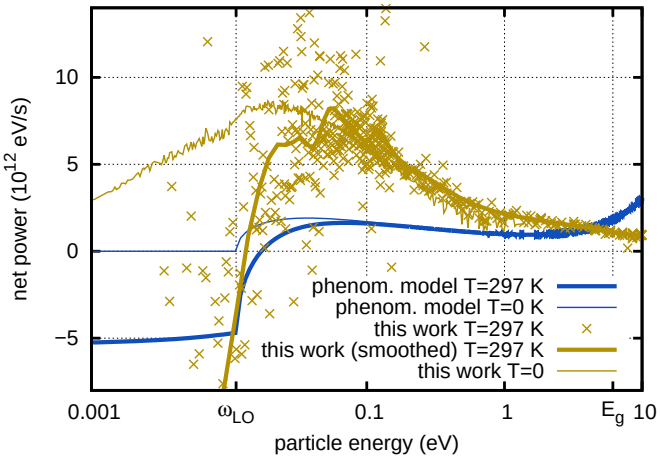

FIG. 7: (Color online) Computed transferred power as a function of particle energy for room and 0 temperature in CsI compared to the phenomenological model from Ref. [13].

It has recently been noted[2,26] that the effective mass approximation predictions for particle velocity ($\mathbf{v}(\mathbf{k}) = \mathbf{k}/m^*$) agree very poorly with those from modern band structure calculations over the energy range of interest. For low-energy electrons in a system with a non-degenerate conduction band such as CsI, there is only one band that can host carriers, and the assignment of the effective mass is unambiguous and can be found reliably from *ab initio* calculations. But, if the particle's energy is great enough (about 0.47 eV above the conduction band minimum in our LDA calculations), there are multiple bands available for the electron, and the assignment of an effective mass to these carriers is ambiguous. Also, at higher energies, the computed bands are generally much shallower than the effective mass approximation (leading

to much higher effective masses). This can be understood by noting that while the electron Bloch states are eigenstates of the crystal momentum $\mathbf{k}$ they are not eigenstates of the total momentum $\mathbf{k}+\mathbf{G}$. Instead, the Bloch states contain higher Fourier components with total momentum contributions in different directions. Therefore, the expectation value of the momentum operator will experience vector cancellation of the momentum states and tend to systematically underestimate the magnitude of the momentum of individual measurements. As a consequence, for higher energy bands, the dispersion $E(\mathbf{k})$ will not be expected to adequately describe the dynamics of particles propagating with a wavepacket largely composed of a narrow spread of momenta.

It is worth noting that the methods presented here can be used not only for electrons, but also for charged nuclear particle radiation such as protons, alpha particles, and recoil ions. In this case, the approximation of using classical motion for the particle is expected to be less problematic. Back of the envelope estimates based on the Rutherford scattering cross-section suggest that our approximations will be valid for heavy ions of high energy (with small scattering angles). For slow, heavy ions, our approximations are expected to break down as the average scattering angle increases. Specifically, high angle scattering is important for low-energy projectiles which experience greater momentum transfers than swift particles. A rough criteria for the sufficiency of the grid upon which the scattering potential is tabulated is that, in atomic units, the product of energy cut-off that defines the plane-wave grid and the projectile energy (in atomic units) be greater than the ratio of the mass of the projectile to that of an electron. At the same energy scale (and for related reasons) the pseudopotential approximation will also become suspect. The neglect of multi-phonon processes also is not applicable to slow, heavy ions since the typical energy transfer for collisions involving such particles exceeds the phonon energies. We find that the single phonon approximation is valid when the ratio of the projectile mass to the average mass of the nuclei in the material is much less than the product of the projectile energy and a representative phonon frequency. Finally, slow, heavy ions are likely to be screened by electrons in the material, and the current formulation does not account for this important process.

VI. CONCLUSIONS

We have used detailed band structure calculations to directly compute the density response to phonon excitation in CsI and used these results to estimate the power by which a charged particle moving through the material is slowed. Our results show significantly higher power, especially for acoustic modes, than the conventional models. We suggest that thermalization time and distance estimates be reassessed. We find that the dispersion relation for quasiparticles has a significant effect on the rate at which energy is lost by a quasiparticle. The discrepancy between the dispersion resulting from band structure calculations and the ubiquitous effective mass approximation poses a serious challenge to the effort to update classic phenomenological models with first-principles numerical models. A coherent picture that recovers the standard models of electron-phonon interaction has not yet been found. Experimental insight into quasiparticle motion and scattering by phonons would be very valuable to illuminate the microscopic physics of these important processes. We plan to use various descriptions of phonon scattering and quasiparticle dispersion in an attempt to improve our models of inorganic scintillators, but more direct experimental insight into the electron-phonon interaction would be very welcome.

VII. ACKNOWLEDGMENTS

This research was supported by the National Nuclear Security Administration, Office of Defense Nuclear Nonproliferation Research and Development (DNN R&D), of the U.S. Department of Energy (DOE). A portion of the research was performed using PNNL Institutional Computing at Pacific Northwest National Laboratory (PNNL). PNNL is a multiprogram national laboratory operated by Battelle Memorial Institute for the U.S. DOE under contract DE-AC0576RL01830.

* Electronic address: micah.prange@pnnl.gov

[1] R. Devanathan, L. Corrales, F. Gao, and W. Weber, Nuc. Instrum. and Methods in Physics Research Section A: Accelerators, Spectrometers, Detectors and Associated Equipment **565**, 637 (2006).
[2] Q. Li, J. Q. Grim, K. B. Ucer, A. Burger, G. A. Bizarri, W. W. Moses, and R. T. Williams, phys. status solidi (RRL) – Rapid Research Letters **6**, 346 (2012).
[3] Q. Li, J. Q. Grim, R. T. Williams, G. A. Bizarri, and W. W. Moses, J. Appl. Phys. **109**, 123716 (2011).
[4] W. Moses, G. Bizarri, R. Williams, S. Payne, A. Vasil'ev, J. Singh, Q. Li, J. Grim, and W. Choong, IEEE Trans. Nucl. Sci. **59**, 2038 (2012).
[5] S. Payne, N. Cherepy, G. Hull, J. Valentine, W. Moses, and W.-S. Choong, IEEE Trans. Nucl. Sci. **56**, 2506 (2009).
[6] W. Setyawan, R. M. Gaume, R. Feigelson, and S. Curtarolo, IEEE Trans. Nucl. Sci. **56**, 2989 (2009).
[7] A. Vasil'ev, IEEE Trans. Nucl. Sci. **55**, 1054 (2008).
[8] G. Bizarri and P. Dorenbos, Phys. Rev. B **75**, 184302 (2007).
[9] A. Canning, A. Chaudhry, R. Boutchko, and N. Grønbech-Jensen, Phys. Rev. B **83**, 125115 (2011).

[10] P. Erhart, A. Schleife, B. Sadigh, and D. Åberg, Phys. Rev. B **89**, 075132 (2014).

[11] G. Bizarri, W. Moses, J. Singh, A. Vasil'ev, and R. Williams, J. Lumin. **129**, 1790 (2009).

[12] S. Kerisit, K. M. Rosso, B. D. Cannon, F. Gao, and Y. Xie, J. Appl. Phys. **105**, 114915 (2009).

[13] Z. Wang, Y. Xie, L. W. Campbell, F. Gao, and S. Kerisit, J. Appl. Phys. **112**, 014906 (2012).

[14] Z. Wang, Y. Xie, B. D. Cannon, L. W. Campbell, F. Gao, and S. Kerisit, J. Appl. Phys. **110**, 064903 (pages 10) (2011).

[15] H. Frohlich, Proc. R. Soc. of London. A **160**, 230 (1937).

[16] J. Ziman, *Electrons and Phonons: The Theory of Transport Phenomena in Solids*, The international series of monographs on physics (Clarendon Press, 1996).

[17] D. Pines, *Elementary Excitations In Solids*, Advanced Book Classics (Westview Press, 1999).

[18] R. P. Feynman, Phys. Rev. **97**, 660 (1955).

[19] G. Mahan, *Many-Particle Physics*, Physics of Solids and Liquids (Springer, 2000).

[20] A. Belsky, K. Ivanovskikh, A. Vasil'ev, M.-F. Joubert, and C. Dujardin, J. Phys. Chem. Letters **4**, 3534 (2013).

[21] F. Quéré, S. Guizard, P. Martin, G. Petite, H. Merdji, B. Carré, J.-F. Hergott, and L. Le Déroff, Phys. Rev. B **61**, 9883 (2000).

[22] M. Sparks, D. L. Mills, R. Warren, T. Holstein, A. A. Maradudin, L. J. Sham, E. Loh, and D. F. King, Phys. Rev. B **24**, 3519 (1981).

[23] A. Akkerman, T. Boutboul, A. Breskin, R. Chechik, and A. Gibrekhterman, J. Appl. Phys. **76**, 4656 (1994).

[24] J. Llacer and E. L. Garwin, J. Appl. Phys. **40**, 2766 (1969).

[25] F. Gao, Y. L. Xie, Z. G. Wang, S. Kerisit, D. X. Wu, L. W. Campbell, R. M. Van Ginhoven, and M. Prange, J. Appl. Phys. **114**, 173512 (2013).

[26] M. Prange, D. X. Wu, Y. L. Xie, L. W. Campbell, S. Kerisit, F. Gao, in Proc. SPIE 9213, Hard X-Ray, Gamma-Ray, and Neutron Detector Physics XVI, 92130L (2014).

[27] X. Gonze, Phys. Rev. B **55**, 10337 (1997).

[28] X. Gonze and C. Lee, Phys. Rev. B **55**, 10355 (1997).

[29] X. Gonze, B. Amadon, P.-M. Anglade, J.-M. Beuken, F. Bottin, P. Boulanger, F. Bruneval, D. Caliste, R. Caracas, M. Côté, et al., Comput. Phys. Commun. **180**, 2582 (2009).

[30] X. Gonze, J.-M. Beuken, R. Caracas, F. Detraux, M. Fuchs, G.-M. Rignanese, L. Sindic, M. Verstraete, G. Zerah, F. Jollet, et al., Computational Materials Science **25**, 478 (2002).

[31] G. Lehmann and M. Taut, phys. status solidi (b) **54**, 469 (1972).

[32] N. Troullier and J. L. Martins, Phys. Rev. B **43**, 1993 (1991).

[33] S. Goedecker, M. Teter, and J. Hutter, Phys. Rev. B **54**, 1703 (1996).

[34] Ganesan, S., Burstein, E., Karo, A.M., and Hardy, J.R., J. Phys. France **26**, 639 (1965).

[35] J. Bardeen and W. Shockley, Phys. Rev. **80**, 72 (1950).

[36] M. Born and K. Huang, *Dynamical Theory of Crystal Lattices* (Oxford University Press, USA, 1998).

[37] R. P. Feynman, R. W. Hellwarth, C. K. Iddings, and P. M. Platzman, Phys. Rev. **127**, 1004 (1962).